Structural Equilibrium Fluctuations in Mesophilic and Thermophilic α-Amylase

J. Fitter*† and J. Heberle*

*Forschungszentrum Jülich, IBI-2, Biologische Strukturforschung, D-52425 Jülich, and †Technische Universität Darmstadt, Institut für Biochemie, D-64287 Darmstadt, Germany

ABSTRACT By comparing a mesophilic α-amylase with its thermophilic homolog, we investigated the relationship between thermal stability and internal equilibrium fluctuations. Fourier transform infrared spectroscopy monitoring hydrogen/deuterium (H/D) exchange kinetics and incoherent neutron scattering measuring picosecond dynamics were used to study dynamic features of the folded state at room temperature. Fairly similar rates of slowly exchanging amide protons indicate about the same free energy of stabilization ΔG_{stab} for both enzymes at room temperature. With respect to motions on shorter time scales, the thermophilic enzyme is characterized by an unexpected higher structural flexibility as compared to the mesophilic counterpart. In particular, the picosecond dynamics revealed a higher degree of conformational freedom for the thermophilic α-amylase. The mechanism proposed for increasing thermal stability in the present case is characterized by entropic stabilization and by flattening of the curvature of ΔG_{stab} as a function of temperature.

INTRODUCTION

Thermophilic organisms grow optimally at temperatures above 60–70°C (Adams and Kelly, 1995; Madigan and Marrs, 1997). This requires proteins that remain folded and functional at high temperatures (often called thermoenzymes). It is known from many studies on a variety of protein structures that besides other environmental conditions (hydration state, pH, or ion concentration), temperature exerts a profound influence on the balanced interplay of structural flexibility and rigidity. A sufficient structural rigidity preserving the specific and unique fold of a protein structure, on the one hand, is as important as sufficient internal conformational flexibility required for proper function (enzymatic activity for example), on the other hand. Therefore, thermoenzymes are not only characterized by a high thermal stability but, in general, also by a higher temperature of maximum enzymatic activity as compared to their mesophilic analogs (thermal adaptation) (Jaenicke et al., 1996; Zavodszky et al., 1998). Because of these characteristics, thermoenzymes are remarkable tools for studying protein stability. For globular (mesophilic) proteins the free energy of stabilization (ΔG_{stab}) is typically 30–65 kJ/mol at room temperature (Privalov, 1979), which is comparable to that of a few hydrogen bonds. As known from only a few ΔG_{stab} values determined for thermoenzymes so far, their ΔG_{stab} is larger as compared to mesophilic species with differences in stabilization energies (between mesophilic and thermophilic species) $\Delta\Delta G_{stab}$ of ~30–50 kJ/mol (Jaenicke, 1996; Beadle et al., 1999). On the other hand, there is no stringent condition that thermophilic enzymes have a larger ΔG_{stab} at room temperature than their mesophilic counterparts. However, there is a long-standing debate about the reasons and mechanisms of enhanced thermostability in thermoenzymes (see, for example, Vielle and Zeikus, 1996; Ladenstein and Antranikian, 1998). With respect to the complexity of a protein structure, it seems improbable that only one universal stabilization mechanism is responsible for thermostability. In fact, many stabilization features have been identified by comparing crystal structures from thermoenzymes and the mesophilic analogs (see, for example, Vielle and Zeikus, 1996; Ladenstein and Antranikian, 1998, and references therein). Among them, additional hydrogen bonds, additional salt bridges, increased internal hydrophobicity, shortening of loops, and conformational strain release are supposed to play a major role in increasing thermostability. It is assumed that one of the main effects of these stabilization features is to increase the rigidity of the protein structure (Vielle and Zeikus, 1996; Madigan and Marrs, 1997; Zavodszky et al., 1998). The reduced conformational flexibility of loop regions, of secondary structure elements, or of the core region is supposed to make the protein structure less susceptible to thermal unfolding. Therefore, thermoenzymes are expected to be less flexible compared to their mesophilic analogs. In several recent studies the dynamic properties of enzymes with different thermostabilities (thermoenzymes, thermostable mutants, and their mesophilic analogs) have been compared, mainly by techniques monitoring hydrogen/deuterium (H/D) exchange kinetics and by molecular dynamics simulations. Some of these studies do support the idea of less flexible thermoenzymes (Zavodszky et al., 1998; de Jongh et al., 1995; Tang and Dill, 1998), while some do not (Jung et al., 1997; Yamasaki et al., 1998; Colombo and Merz, 1999; Hernandez et al., 2000). Although protein dynamics is characterized by motions on a broad spectrum of different time scales, not all time scales need to be relevant or significant for stability. There is not a unique or specific correlation per se between thermal stability and structural

Received for publication 15 March 2000 and in final form 22 May 2000.

Address reprint requests to Dr. Joerg Fitter, Forschungszentrum Jülich, IBI-2, Biologische Strukturforschung, D-52425 Jülich, Germany. Tel.: +49-2461-61-2036; Fax: +49-2461-61-2020; E-mail: j.fitter@fz-juelich.de.

0006-3495/00/09/1629/08 $2.00

fluctuation. Nevertheless, various interactions are possible and have been confirmed in some cases. An increased number of stabilizing salt bridges or additional hydrogen bonds is often accompanied by reduced B-factors and smaller accessible surface areas, indicating a reduced flexibility due to a larger compactness and stiffness of the protein structure (Wallon et al., 1997; Korndorfer et al., 1995). On the other hand, structural flexibility observed through equilibrium fluctuations contributes to the conformational entropy and to the entropy change during unfolding ΔS and may have a profound influence on the free energy of stabilization (Matthews et al., 1987; Lazaridis et al., 1997). However, more experimental data are required to determine whether and how structural fluctuations are related to thermostability and to thermal adaptation. A promising approach to improving the knowledge of the physical basis of protein stability is to compare dynamic features of mesophilic proteins and their thermophilic homologs, which share a high sequence identity and structural similarity but are greatly different in terms of thermostability (Jaenicke et al., 1996; Lazaridis et al., 1997). Following this strategy, we have studied the dynamic characteristics of two α-amylases. With Fourier transform infrared (FT-IR) spectroscopy we measured the H/D exchange kinetics, which is related to local and global conformational fluctuations occurring on a long time scale. In addition, incoherent neutron scattering (INS) was used to monitor mainly local equilibrium fluctuations on the picosecond time scale. It is the purpose of this paper to present results from dynamic behavior as measured with both α-amylases on very different time scales and to discuss them with respect to thermostability.

MATERIALS AND METHODS

Thermostable α-amylase and the mesophilic homolog

α-Amylases catalyze the cleavage of $\alpha\rightarrow$D-(1$\rightarrow$4) glycosidic bonds in starch and related carbohydrates. Because starch is most soluble at high temperatures, thermostable enzymes play a key role in industrial hydrolysis. Although the organism *Bacillus licheniformis* itself is not a thermophile, it contains a rather thermostable α-amylase (BLA) (Vihinen and Mäntsälä, 1989). The three-dimensional structure of BLA has been determined to atomic resolution by x-ray crystallography (Machius et al., 1995, 1998). BLA is a monomer of ~58 kDa exhibiting an α/β-barrel as a central part (see Fig. 1). As a mesophilic homolog, α-amylase from *Bacillus amyloliquefaciens* (BAA), with nearly the same molecular mass (58 kDa) as BLA, was chosen. Sequence alignment of BLA and BAA performed by Machius and co-workers (Machius et al., 1995) revealed a very high homology (81% identity, 88% similarity). Although the crystal structure of BAA has not yet been determined, the sequence alignment and the comparison of FT-IR spectra suggests that the three-dimensional structures of BAA can be expected to be rather similar to those of BLA (according to the amide I component bands in the FT-IR spectra (see, for example, Byler and Susi, 1986), the compositions of secondary structure elements of the two α-amylases are very similar; data not shown). It is well known that the calcium concentration greatly influences the stability of α-amylases (Violet and Meunier, 1989; Declerck et al., 1997; Machius et al., 1998). While the addition of $CaCl_2$ increases the temperature of thermal unfolding T_m (by ~25°C in the case of BLA and BAA), the addition of chelators (like EDTA) decreases T_m significantly (Violet and Meunier, 1989; Declerck et al., 1997; Feller et al., 1999). Nevertheless, under similar conditions (i.e., both enzymes with or without $CaCl_2$) BLA exhibits a T_m value that is ~20°C larger compared to that of BAA. In phosphate buffer, as used for measurements presented in this paper, we have determined that $T_m = 55$°C for BAA and $T_m = 76$°C for BLA (Fitter et al., manuscript in preparation). In a first series of measurements, α- amylase samples were kept at neutral pH, without additional ions (in particular, Ca^{2+} ions), and the measurements were performed at room temperature.

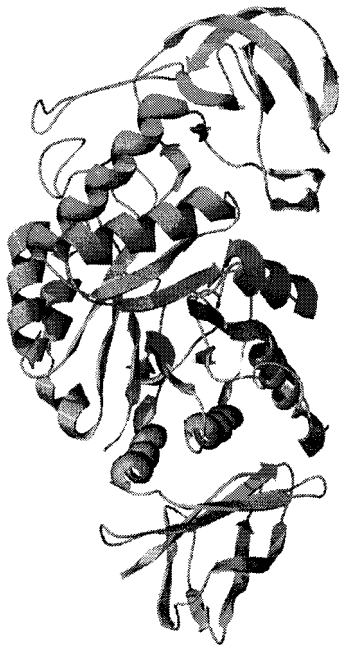

FIGURE 1 Crystal structure of α-amylase from *Bac. licheniformis* (PDB-entry:1BLI). The structure is characterized by three distinct domains, a central (α/β) barrel (domain A), domain B (upper part of the structure), and domain C (lower part).

Infrared spectroscopy

Sample preparation for FT-IR spectroscopy was identical for α-amylase from *Bacillus licheniformis* (purchased from Sigma-Aldrich) and from *Bac. amyloliquefaciens* (purchased from Fluka). Lyophilized α-amylase (3.8 mg) was dissolved in 150 μl D_2O buffer (50 mM phosphate buffer, pH 7.4). From this solution (enzyme concentration 25 mg/ml) 6 μl was put in a homemade thermostatted cell, equipped with CaF_2 windows providing a light pathlength of ~45 μm. Spectra were measured on a Bruker Vector 22 FT-IR spectrometer, using a DTGS detector. A series of spectra ranging from 0 to 7000 cm^{-1} was recorded starting ~2 min after the lyophilized enzyme was dissolved in D_2O buffer. During the first 20 min 10 scans were acquired, at intervals of 2 min. Subsequently, 60 scans were performed every 20 min. Spectra were recorded at $T = 20$°C or at $T = 30$°C, with a spectral resolution of 4 cm^{-1}. Protein aggregation was not observed for samples at the given protein concentration of ~25 mg/ml during the whole time of our measurements. (For BAA samples at higher protein concentrations (50 mg/ml) and for $T \geq 30$°C we observed after ~6 h of incubation an additional intensity around 1600 cm^{-1} that is typical for protein aggregation.) To determine the fraction of exchanged amide protons, measurements with enzyme in H_2O solvent (sample with nonexchanged protons) and further measurements of fully exchanged amide protons were per-

formed at both temperatures. For samples in H_2O buffer, a cell with a pathlength of 10 μm was used. Samples with fully exchanged amide protons were obtained by storing the enzyme in D_2O buffer for ~4 weeks at ~30°C. Because of protein precipitation during the long incubation time, the solution was briefly centrifuged (13,000 rpm) for 5 min to remove aggregated protein. After subtraction of pure buffer spectra from the spectra of α-amylase solution, the absorbances at amide I (A_I) and amide II (A_{II}) were evaluated from intensities in the wavelength range from 1647 to 1651 cm^{-1} and from 1545 to 1549 cm^{-1}, respectively. Considering slight variations of protein concentrations in the light path during the measurements and/or between different samples, the time-dependent intensities of amide II were normalized using the amide I band:

$$I(t) = \frac{A_{II}}{A_I}. \tag{1}$$

The fraction of nonexchanged amide protons can be calculated by

$$F(t) = \frac{I(t) - I(\infty)}{I(0) - I(\infty)}, \tag{2}$$

where $I(\infty)$ is the amide II/amide I ratio as determined with fully exchanged samples, and $I(0)$ was calculated from intensities as measured with samples in H_2O buffer (100% nonexchanged). The results were confirmed by two additional and independent measurements at two temperatures. The decay of $F(t)$ for both samples and for both temperatures was fitted with two exponentials. The first exponential is characterized by a lifetime between 30 and 80 min. The second exponential revealed much longer lifetimes of ~100 h. Because we have measured H/D exchange only up to 20 h, the lifetimes obtained for the second exponential are very sensitive to the curvature of the data in the region between 400 and 1200 min. Because even small errors in the measured data points change the obtained lifetime drastically, we performed a linear fit in this region. The exchange rates obtained from the linear fit were used in a subsequent fit with two exponentials but were kept fixed. The result of this procedure was quite reasonable; this is shown in Fig. 4.

Incoherent neutron scattering

As already emphasized for the FT-IR measurements, sample preparation for neutron scattering measurements has been performed identically and in parallel for the two α-amylases. Lyophilized enzyme (125 mg) was dissolved in 2.5 ml of D_2O buffer (50 mM phosphate buffer, pH 7.4). After the solution was stirred for 30 s at room temperature (25°C), the enzyme was completely dissolved. Two milliliters of solution (enzyme concentration 50 mg/ml) was put in a slab-shaped aluminum sample container (inner sample volume 40 mm (width) × 50 mm (height) × 1 mm (thickness)) and was finally closed with a cap with a Teflon ring seal. Neutron scattering experiments have been carried out using the time-of-flight spectrometer IN6 (Institute Laue-Langevin, Grenoble). Each sample was measured for ~5 h, ensuring counting statistics good enough to perform a reasonable data analysis. The time-of-flight spectra were measured and corrected as described elsewhere (Fitter, 1999). Relatively large transmission values of $T(90°) \approx 0.90–0.95$ made it possible to perform a data analysis without correcting for multiple scattering. It was necessary to subtract solvent scattering, because it represents about two-thirds of the total scattering from the α-amylase samples (Fig. 2 *a*). The obtained difference spectra (see Fig. 2 *b*) are characterized mainly by incoherent scattering from nonexchangeable H atoms of α-amylase. In a neutron scattering experiment with predominantly incoherent scattering, the double-differential cross section

$$\frac{\delta^2\sigma}{\delta\Omega\ \delta\omega} = \frac{1}{4\pi} \cdot \frac{|\mathbf{k}_1|}{|\mathbf{k}_0|} \cdot [b_{inc}^2 \cdot S_{inc}(\mathbf{Q}, \omega)] \tag{3}$$

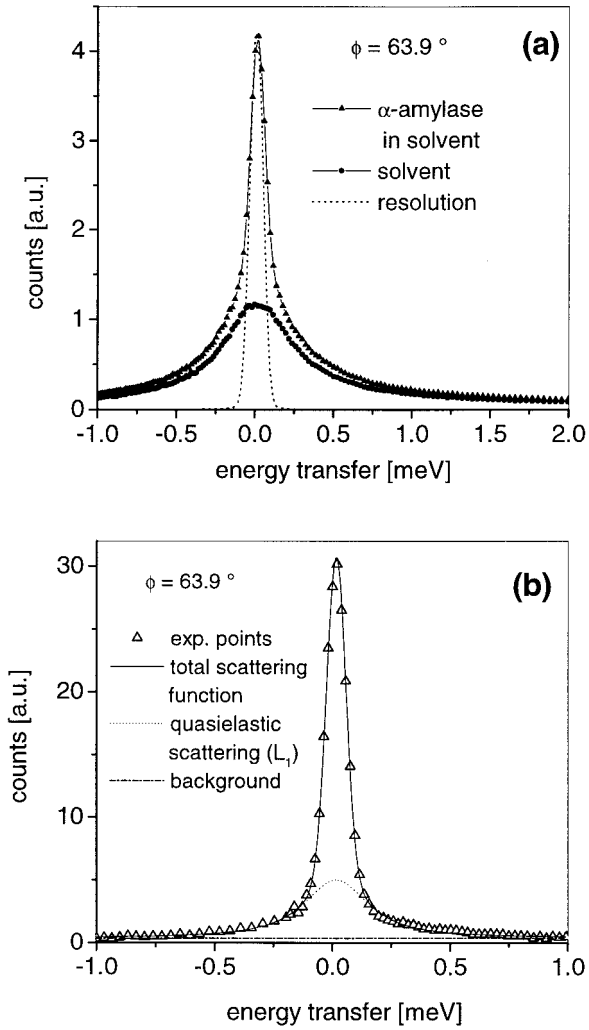

FIGURE 2 Steps in the data analysis of α-amylase in D_2O solution. (*a*) Comparison of spectra as measured with enzyme solution (▲) and with pure buffer only (●). At the given scattering angle $\phi = 63.9°$ the solvent scattering is about two-thirds of the total scattering observed for enzyme solutions. (*b*) The difference spectrum (enzyme solution minus solvent as shown in *a*) at the given scattering angle ϕ has been fitted with an elastic contribution, a single Lorentzian (L_1, with $H_1 = 150$ μeV), and a linear background.

determines the number of neutrons scattered into a solid angle element $\delta\Omega$ and an energy transfer element $\delta\omega$. Here b_{inc} denotes the incoherent scattering length, and $\mathbf{k}_0$ and $\mathbf{k}_1$ are the wave vectors for the incident and scattered neutrons, respectively (with momentum transfer $\mathbf{Q} = \mathbf{k}_1 - \mathbf{k}_0$). The obtained spectra, which were grouped from the original 234 spectra into 22 spectra, were fitted using

$$S_{meas}(\mathbf{Q}, \omega) = F \cdot e^{-\hbar\omega/2k_BT} \cdot [S_{theor}(\mathbf{Q}, \omega) \otimes S_{res}(\mathbf{Q}, \omega)] + B, \tag{4}$$

applying a convolution (⊗, energy convolution operator) with the resolution function $S_{res}(Q,\omega)$ (obtained from vanadium measurements). F denotes a normalization factor, and $\exp(-\hbar\omega/2k_BT)$ gives the detailed balance factor. B is a linear and constant background. For localized motions the theoretical incoherent scattering function $S_{theor}(Q,\omega)$ in general form is

given by

$$S_{\text{theor}}(\mathbf{Q}, \omega) = e^{-\langle u^2\rangle Q^2} \cdot \left[A_0(\mathbf{Q}) \cdot \delta(\omega) + \sum_{i=1}^{n} A_i(\mathbf{Q}) \cdot L_i(H_i, \omega) \right]. \quad (5)$$

The scattered intensity is separated into an elastic $\delta(\omega)$-shaped component (experimentally observed with the resolution width Γ_{res}) and the quasielastic Lorentzian-shaped contribution $L_i(H_i,\omega)$, parameterized by the width $H_i = (\tau_i)^{-1}$ (τ_i is the corresponding correlation time) and by the quasielastic incoherent structure factor A_i. The intensity of the elastic component is given by the elastic incoherent structure factor A_0. Faster motions are taken into account by the Debye-Waller factor, $\exp(-\langle u^2\rangle \cdot Q^2)$, where $\langle u^2\rangle$ gives the global average "mean square displacements" of vibrational motions of all protons. To compare characteristic dynamic features of the two enzymes, a simple model describing a "diffusion inside a sphere" was applied. This model is characterized by the following elastic incoherent structure factor (Volino and Dianoux, 1980):

$$A_0(Q) = \left[3 \frac{\sin(Qr_{sp}) - (Qr_{sp}) \cdot \cos(Qr_{sp})}{(Qr_{sp})^3} \right]^2. \quad (6)$$

Because our data are limited in momentum transfer Q (with $Q_{max} = 2.25$ Å) and in energy transfer with $|\hbar\cdot\omega| \leq 1.0$ meV, only the first quasielastic component ($A_1 = 1 - A_0$) was considered. Therefore, the theoretical scattering function

$$S_{\text{theor}}(Q, \omega) = e^{-\langle u^2\rangle Q^2} \cdot [(1 - f_{sp} + f_{sp} \cdot A_0(Q)) \cdot \delta(\omega) + f_{sp} \cdot A_1(Q) \cdot (L_1(H_1, \omega)] \quad (7)$$

is parameterized by the radius of the sphere r_{sp}, the fraction f_{sp} (both determining A_0 and A_1), and the width of the quasielastic contributions $H_1 = (\tau_1)^{-1}$. With respect to the time range considered in the applied data analysis (~10 ps to ~0.3 ps), f_{sp} gives the fraction of protons participating in localized diffusion. Protons that are too slow to be resolved in our measurements are represented by the factor $(1 - f_{sp})$. As shown in Fig. 2 *b*, an elastic contribution, a single Lorentzian ($H_1 = 150$ μeV), and a linear background were sufficient to fit the spectra in the given energy transfer range. First, in phenomenological fits all spectra were fitted separately (see Eq. 5) to determine the "experimental" A_0. To quantify the parameters r_{sp} and f_{sp}, all spectra were fitted simultaneously (Eq. 7). Small and systematic deviations between "experimental" and model A_0 (see Fig. 5 *b*) are typical for multiple scattering effects. For further methodical details, see, for example, Fitter et al. (1997, 1998). It is noteworthy that in the case of biological macromolecules the correlation times τ and radii r must be understood as averaged parameters, describing a much more complex dynamic behavior observable in the time window of our experiments (a few picoseconds).

RESULTS

Both techniques applied in the present study, H/D exchange kinetics and incoherent neutron scattering, give insight into the ("overall") internal molecular flexibility of the protein structures by monitoring thermal equilibrium fluctuations. While INS observes fast (femto- to picosecond time scale) stochastic local, general noncooperative rearrangements of structural segments (e.g., polypeptide side chains), H/D exchange is in principle related to the same type of motion but needs more cooperativity and therefore occurs much less frequently (minutes to hours).

Amide-proton exchange kinetics

Initially buried segments of the polypeptide chain will be progressively exposed to the solvent with time because of thermal equilibrium fluctuations. If a lyophilized protein is dissolved in D_2O, H/D exchange occurs during such exposure. With respect to FT-IR spectroscopy, amide protons are visible in the amide II band (around 1550 cm^{-1}) of the IR spectrum, which corresponds to the N-H in-plane bending mode strongly coupled to the C═N stretching vibration (Susi, 1972). Amide protons localized at the surface of a protein exchange very fast. Those amide protons that exchange much more slowly are involved in structure stabilization and are buried deeper (Hvidt and Nielsen, 1966; Pershina and Hvidt, 1974). As shown in Fig. 3, H/D exchange decreases the absorbance of the amide II band. The concurrent increasing in N-D bending is related to an increase in absorbance at 1450 cm^{-1} (amide II′, overlapped by HDO absorbance). A typical series of spectra (measured with BLA at 30°C, shown in Fig. 3) reflects the time course of H/D exchange. The absorbance of amide I at 1650 cm^{-1}, which arises from C═O in-plane stretching vibrations of the protein backbone (Susi, 1972), is hardly influenced by H/D exchange. Therefore, the amide I band is generally used for the normalization of amide II. The fraction of nonexchanged amide protons as a function of time is plotted

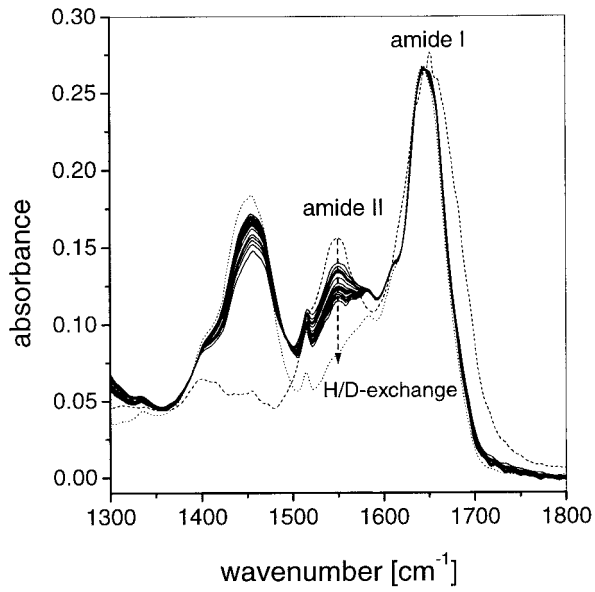

FIGURE 3 Series of FT-IR spectra of BLA at 30°C in D_2O. The H/D exchange is observable by a decrease in absorbance of the amide II band. All spectra were normalized to the amide I intensity. The dashed line represents a spectrum measured with H_2O solvent (100% nonexchanged). The dotted line is a spectrum of the sample with fully exchanged amide protons.

in Fig. 4. The H/D exchange was measured over 20 h at 20°C and at 30°C for both enzymes. As already found for other proteins, all amide protons can be roughly divided into three different classes (Kim et al., 1993; de Jongh et al., 1995). Initially, fast exchanging protons (class I) are observed that are exposed to the surface or located in loop regions, making them accessible to solvent molecules. Nearly all amide protons from this fraction are exchanged after ~30 min. Most of these protons are not resolved in our measurements because the first spectrum is recorded 2 min after the enzyme is dissolved in D_2O. Another class of amide protons exchanging with intermediate rates (class II) is located in flexible buried regions or in secondary structure elements that are not part of the core region. A slowly exchanging fraction (class III) is related to amide protons located predominantly in the core region of the protein. With respect to this classification we have fitted the time dependence of H/D exchange with two exponentials (describing the decay of class II and III protons); the results are given in Table 1.

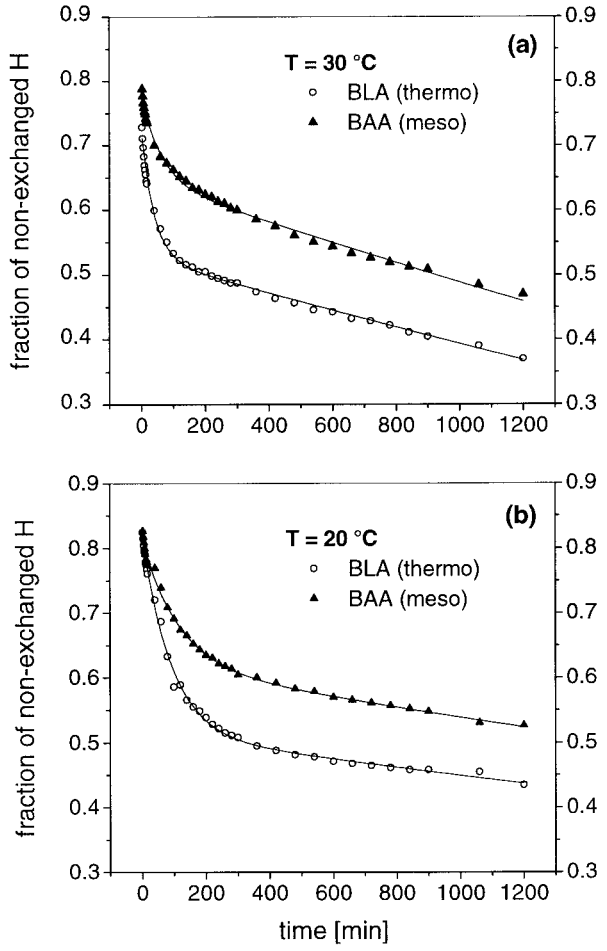

FIGURE 4 Normalized fractions of nonexchanged amide protons as a function of exposure time measured with BLA and with BAA at 30°C (*a*) and 20°C (*b*). The experimental points have been obtained from amide II intensities as detected by FT-IR spectroscopy (Fig. 3). The solid lines represent two-exponential fits to the data points. The resulting parameters are given in Table 1.

The most striking result is a significantly faster and more complete H/D exchange of class II protons in BLA as compared to BAA (Fig. 4 and Table 1). In contrast to this, the fractions and the exchange rates of the slowly exchanging protons (class III) and the fractions of the fast exchanging protons (class I) are rather similar for the two α-amylases. With respect to the difference between BLA and BAA, the H/D exchange is qualitatively similar for the two temperatures. The temperature dependence is characterized by a larger fraction of exchanged protons for $T = 30$°C as compared to 20°C for class I and class III protons. For the lower temperature we observe smaller exchange rates for class II and class III protons. According to H/D exchange studies using NMR spectroscopy, the fraction of slowly exchanging amide protons is mainly related to cooperative transient unfolding motions. Therefore, exchange rates from this fraction are used to determine ΔG_{stab} (Mayo and Baldwin, 1993; Kim et al., 1993). Interestingly, our observations indicate a free energy of stabilization that is rather similar for the two enzymes. In contrast to this, local noncooperative motions represented by intermediate exchange rates (class II) are not related to the global stability (Kim and Woodward, 1993). Fractions of exchanged class II amide protons as well as corresponding exchange rates are larger by a factor of ~1.5 for BLA as compared to BAA (for class III protons this factor is ~1.0–1.1). This result indicates that these motions are more pronounced in the thermostable BLA, which shows more local fluctuations than BAA. With respect to our data, a precise separation between protons related to the class I and class II processes is difficult (see Materials and Methods). Therefore, the observed difference in the behavior of class II protons between BAA and BLA may also be influenced by proton exchange of class I due to the different fraction of easily accessible backbone amide protons on the surface or in loops.

Picosecond fluctuations studied by incoherent neutron scattering

Incoherent neutron scattering makes use of a large incoherent cross section of hydrogen nuclei (~40 times larger than incoherent cross sections of other elements in biological samples) and is well suited to the study of internal molecular motions in a time range from 10^{-9} to 10^{-14} s. With the enzymes dissolved in D_2O, all nonexchangeable hydrogens (~3400 per molecule of BLA or BAA, which are distributed "quasihomogeneously" in the molecule) serve as probes to monitor local fluctuations occurring in the structure. In a neutron scattering experiment with predominantly incoherent scattering, information on the dynamics of individual hydrogen atoms can be obtained from the incoherent scattering function $S_{inc}(Q, \omega)$, using the formalism of self-correlation functions. According to the diffusive and liquid-

TABLE 1 Results from H/D exchange kinetics

		BLA (thermo)		BAA (meso)	
	Class	Fraction of exchanged H	Exchange rates ($10^{-2} * min^{-1}$)	Fraction of exchanged H	Exchange rates ($10^{-2} * min^{-1}$)
T = 30°C	I	0.27	—	0.22	—
	II	0.19	2.43	0.13	1.35
	III	0.21	0.011	0.19	0.010
	Σ	0.67		0.54	
T = 20°C	I	0.18	—	0.18	—
	II	0.29	1.11	0.20	0.88
	III	0.09	0.0062	0.10	0.0071
	Σ	0.56		0.48	

The decay of amide protons (see Fig. 4) from classes II and III has been fitted with two exponentials. Because of the limited time resolution of the measurements (dead time ~2 min), the fractions of exchanged protons represented by class I are directly obtained from the experimental data.

like character of the predominant part of the motions (with samples at physiological conditions), the quasielastic scattering is the focus of our analysis. A comparison of the neutron scattering spectra of BLA and BAA is shown in Fig. 5 *a*. Both spectra represent scattering due to α-amylase only, because scattering from D_2O has been subtracted (see Materials and Methods). As shown in Fig. 5 *a*, we observe a small but significant difference in the quasielastic scattering between BLA and BAA. Only motions with correlation times slower than 0.3 ps exhibit a significant difference between the two enzymes. The intensity of the quasielastic scattering (in the region from τ_c = 6 ps to 0.3 ps) is larger by 10% for the thermophilic BLA sample compared to the mesophilic BAA, indicating a higher conformational flexibility for BLA. To obtain a more quantitative picture of the differences in the dynamic behavior between the two α-amylases, the data were fitted with a specific model. According to the large variety of different structural elements in proteins, only some general properties of the complex dynamic behavior can be reproduced by the simple model applied ("diffusion inside a sphere"). The elastic incoherent structure factor (A_0) is parameterized by the radius of the sphere (r_{sp}), determining a volume explored by the diffusing protons and the fraction of protons participating in this type of motion (f_{sp}). A comparison of the "experimental" elastic incoherent structure factors and A_0 obtained from model fits as a function of Q is given in Fig. 5 *b* (for details see Materials and Methods). Smaller values of A_0 from thermophilic BLA as compared to those of BAA indicate a "higher conformational flexibility," as already observed in Fig. 5 *a*. With respect to both parameters, model fits revealed larger values for the thermophilic BLA (r_{sp} = 2.47 Å, f_{sp} = 0.68) compared to the mesophilic BAA (r_{sp} = 2.23 Å, f_{sp} = 0.63). Within the framework of the applied model, a larger value of r_{sp} implies not only larger amplitudes of motions but also more conformational degrees of freedom due to more possible diffusion sites in a larger volume explored by this type of motion. The observed difference in the quasielastic scattering between

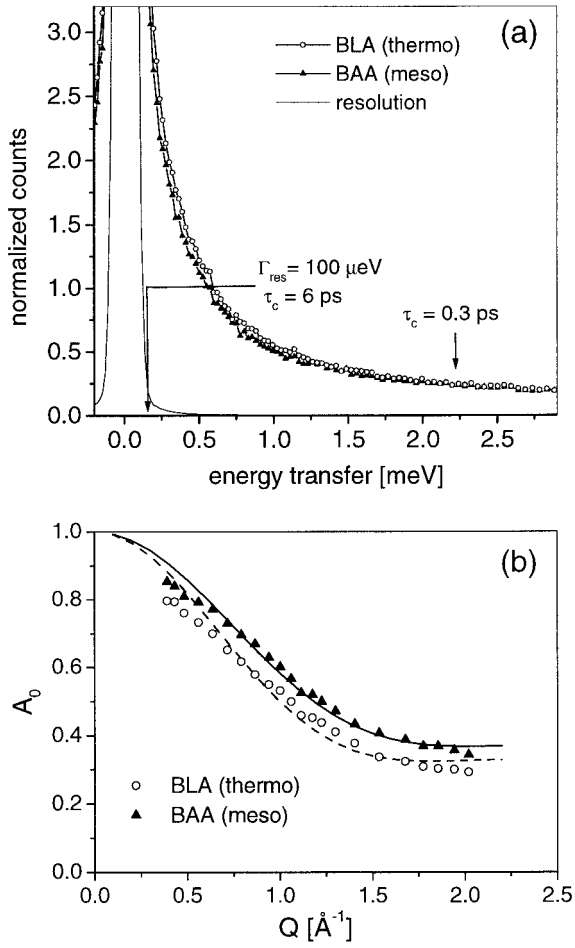

FIGURE 5 (*a*) Incoherent neutron scattering spectra as measured for BLA and for BAA at 30°C (solvent scattering subtracted). The figure represents an enlargement of the quasielastic scattering due to stochastic motions in α-amylase. The top of the frame corresponds to 10% of the elastic peak intensity. (*b*) Elastic incoherent structure factors A_0 as a function of momentum transfer Q. "Experimental" A_0 values (*symbols*) have been determined by phenomenological fits where all spectra were fitted separately. In the case of model fits, all spectra were fitted simultaneously, considering the Q dependence of A_0 as given by the model. *Solid line*, BAA; *dashed line*, BLA.

BLA and BAA has been confirmed by two parallel and independent measurements performed under identical conditions for the two α-amylases. Therefore we can conclude that the thermophilic BLA shows more structural flexibility than the mesophilic BAA.

DISCUSSION

With respect to the limited time scale covered by our measurements and considering that we have studied fluctuations at room temperature only, our results can be summarized by the following statements. Fairly similar rates of the slowly exchanging amide protons observed for both enzymes indicate a thermodynamic stability ΔG_{stab} that is also rather similar for BLA and BAA at room temperature. As supported by faster H/D exchange and by picosecond dynamics, this property is accompanied by a higher structural flexibility of the thermophilic BLA compared to the mesophilic BAA. In most studies comparing H/D exchange in mesophilic enzymes and in thermophilic homologs (or in more stable mutants), a different behavior was observed (Wagner and Wuthrich, 1979; Roder, 1989; de Jongh et al., 1995; Zavodszky et al., 1998). These studies revealed decreasing exchange rates (for slowly exchanging amide protons) by increasing temperatures of unfolding T_m. In accordance with our observation, Yamasaki and co-workers found that an increase in T_m has only little effect on the rates of slowly exchanging amide protons (Yamasaki et al., 1998). The discrepancy among the different studies may result from the fact that different thermostable enzymes use different mechanisms to achieve thermostability. On the other hand, there is some evidence that rates of slowly exchanging amide protons reflect not only unfolding motions but also noncooperative fluctuations that are not related to stability (Kim et al., 1993; Mayo and Baldwin, 1993). However, the most striking observation in our study is a higher flexibility on shorter time scales (fast and intermediate rates of the H/D exchange and picosecond time range) for the thermophilic enzyme. INS studies on the dynamic properties of enzymes in solution are very rare. An INS study on phosphoglycerate kinase (Receveur et al., 1997) reports on a large difference in the picosecond fluctuations between the folded state and the more flexible unfolded state. Compared with these differences, the difference in the dynamical behavior between BLA and BAA is much smaller. Up to now, a comparison of thermophilic-mesophilic pairs with respect to dynamics in the picosecond time regime has been investigated only by molecular dynamics simulations (Lazaridis et al., 1997; Colombo and Merz, 1999). These studies found very similar flexibilities for the two enzymes (or slightly greater flexibility for the mesophilic enzyme; Lazaridis et al., 1997) at room temperature. In contrast to the room temperature behavior, Colombo and co-workers found at elevated temperatures (350 K) a reduced flexibility of mesophilic subtilisin as compared to a thermophilic mutant (Colombo and Merz, 1999). This last observation and differences in the dynamical behavior observed in this study support a possible importance of equilibrium fluctuations for thermostability. In particular, fast fluctuations play a major role in conformational entropy. The free energy of stabilization ΔG_{stab} depends on the balance of enthalpic and entropic contributions. Compared to the native (folded) state, the unfolded state is generally characterized by a much higher degree of conformational freedom. With respect to picosecond fluctuations this property has been observed in an INS study (Receveur et al., 1997). If a high conformational flexibility of the thermophilic BLA is already observed in the native (folded) state, ΔS (entropy change during unfolding) will be smaller, and an entropic stabilization with respect to the less flexible BAA can be found. Because calorimetric data comparing BLA and BAA are not yet available, we propose a qualitative thermodynamic picture of protein stability that is consistent with our observation. A lower ΔS (or a lower ΔC_p, change in specific heat capacity between folded and unfolded states) would increase ΔG_{stab} and/or flatten the parabolic curve describing the temperature dependence of the free energy of stabilization (Becktel and Schellman, 1987). In this case, ΔG_{stab} at room temperature is not necessarily related to the thermal stability. Our example indicates that high thermal stability is mainly achieved by a sufficient residual ΔG_{stab} at high temperatures, while ΔG_{stab} seems to be rather similar for the two enzymes at room temperature. A similar mechanism for increased thermostability was already observed and proposed for other mesophilic-thermophilic pairs (see Beadle et al., 1999, and references therein). Because for different mesophilic-thermophilic pairs different mechanisms of increased thermostability have been found, it is assumed that nature uses different strategies to adapt enzymes to their specific environment. This might explain the differences in dynamic properties between the BAA-BLA pair and the comparison of other mesophilic-thermophilic pairs. To confirm the proposed mechanism for the thermostability of BLA, ongoing and future measurements do and will include studies at different temperatures and with enzymes in the unfolded state.

In the present article we have focused mainly on the thermostability, which is only one of the properties characterizing thermophilic enzymes. Another important property is the elevated temperature of maximum enzymatic activity and generally low enzymatic activity at room temperature (such a behavior was also observed for BLA; Fitter et al., manuscript in preparation). Therefore, an effective thermal adaptation of thermophiles and psychrophiles is characterized by taking into account both aspects. Considering that a proper enzymatic activity requires sufficient conformational fluctuations, the comparison of dynamic features with enzymatic activity is also relevant to understanding thermal adaptation (see, for example, Zavodszky et al., 1998).

We thank the Institute Laue-Langevin (Grenoble, France) for providing neutron beam facilities. D. Heitbrink, C. Bolwien, and D. Hehn are acknowledged for help and support during FT-IR measurements. The authors thank G. Büldt and N. A. Dencher for valuable and stimulating discussions and for continuous and generous support.

This work was supported by grants from the Bundesministerium für Bildung, Wissenschaft, Forschung und Technologie 03-DE5DA1−8 (to JF) and from the Deutsche Forschungsgemeinschaft SFB 189/C5 (to JH).

REFERENCES

Adams, M. W. W., and R. M. Kelly. 1995. Enzymes from microorganisms in extreme environments. *Chem. Eng. News.* 18:32–42.

Beadle, B. M., W. A. Baase, D. B. Wilson, N. R. Gilkes, and B. K. Shoichet. 1999. Comparing the thermodynamic stabilities of a related thermophilic and mesophilic enzyme. *Biochemistry.* 38:2570–2576.

Becktel, W. J., and J. A. Schellman. 1987. Protein stability curves. *Biopolymers.* 26:1859–1877.

Byler, D. M., and H. Susi. 1986. Examination of the secondary structure of proteins by deconvolved FTIR spectra. *Biopolymers.* 25:469–487.

Colombo, G., and K. M. Merz, Jr. 1999. Stability and activity of mesophilic subtilisin E and its thermophilic homolog: insights from molecular dynamics simulations. *J. Am. Chem. Soc.* 121:6895–6903.

Declerck, N., M. Machius, R. Chambert, G. Wiegand, R. Huber, and C. Gaillardin. 1997. Hyperthermostable mutants of *Bacillus licheniformis* alpha-amylase: thermodynamic studies and structural interpretation. *Protein Eng.* 10:541–549.

de Jongh, H. H., E. Goormaghtigh, and J. M. Ruysschaert. 1995. Tertiary stability of native and methionine-80 modified cytochrome *c* detected by proton-deuterium exchange using on-line Fourier transform infrared spectroscopy. *Biochemistry.* 34:172–179.

Feller, G., D. d'Amico, and C. Gerday. 1999. Thermodynamic stability of a cold-active alpha-amylase from the Antarctic bacterium *Alteromonas haloplanctis*. *Biochemistry.* 38:4613–4619.

Fitter, J. 1999. The temperature dependence of internal molecular motions in hydrated and dry alpha-amylase: the role of hydration water in the dynamical transition of proteins. *Biophys. J.* 76:1034–1042.

Fitter, J., R. E. Lechner, and N. A. Dencher. 1997. Picosecond molecular motions in bacteriorhodopsin from neutron scattering. *Biophys. J.* 73: 2126–2137.

Fitter, J., S. A. Verclas, R. E. Lechner, H. Seelert, and N. A. Dencher. 1998. Function and picosecond dynamics of bacteriorhodopsin in purple membrane at different lipidation and hydration. *FEBS Lett.* 433: 321–325.

Hernandez, G., F. E. J. Jenney, M. W. Adams, and D. M. LeMaster. 2000. Millisecond time scale conformational flexibility in a hyperthermophile protein at ambient temperature. *Proc. Natl. Acad. Sci. USA.* 97: 3166–3170.

Hvidt, A., and S. O. Nielsen. 1966. Hydrogen exchange in proteins. *Adv. Protein Chem.* 21:287–386.

Jaenicke, R. 1996. How do proteins acquire their three-dimensional structure and stability? *Naturwissenschaften.* 83:544–554.

Jaenicke, R., H. Schurig, N. Beaucamp, and R. Ostendorp. 1996. Structure and stability of hyperstable proteins: glycolytic enzymes from hyperthermophilic bacterium *Thermotoga maritima*. *Adv. Protein Chem.* 48: 181–269.

Jung, D. H., N. S. Kang, and M. S. Jhon. 1997. Site-directed mutation study on hyperthermostability of rubredoxin from *Pyrococcus furiosus* using molecular dynamics simulations in solution. *J. Phys. Chem. A.* 101: 466–471.

Kim, K. S., J. A. Fuchs, and C. K. Woodward. 1993. Hydrogen exchange identifies native-state motional domains important in protein folding. *Biochemistry.* 32:9600–9608.

Kim, K. S., and C. Woodward. 1993. Protein internal flexibility and global stability: effect of urea on hydrogen exchange rates of bovine pancreatic trypsin inhibitor. *Biochemistry.* 32:9609–9613.

Korndorfer, I., B. Steipe, R. Huber, A. Tomschy, and R. Jaenicke. 1995. The crystal structure of holo-glyceraldehyde-3-phosphate dehydrogenase from the hyperthermophilic bacterium *Thermotoga maritima* at 2.5 Å resolution. *J. Mol. Biol.* 246:511–521.

Ladenstein, R., and G. Antranikian. 1998. Proteins from hyperthermophiles: stability and enzymatic catalysis close to the boiling point of water. *Adv. Biochem. Eng. Biotechnol.* 61:37–85.

Lazaridis, T., I. Lee, and M. Karplus. 1997. Dynamics and unfolding pathways of a hyperthermophilic and a mesophilic rubredoxin. *Protein Sci.* 6:2589–2605.

Machius, M., N. Declerck, R. Huber, and G. Wiegand. 1998. Activation of *Bacillus licheniformis* alpha-amylase through a disorder→order transition of the substrate-binding site mediated by a calcium-sodium-calcium metal triad. *Structure.* 6:281–292.

Machius, M., G. Wiegand, and R. Huber. 1995. Crystal structure of calcium-depleted *Bacillus licheniformis* alpha-amylase at 2.2 Å resolution. *J. Mol. Biol.* 246:545–559.

Madigan, M. T., and B. L. Marrs. 1997. Extremophiles. *Sci. Am.* 276: 82–87.

Matthews, B. W., H. Nicholson, and W. J. Becktel. 1987. Enhanced protein thermostability from site-directed mutations that decrease the entropy of unfolding. *Proc. Natl. Acad. Sci. USA.* 84:6663–6667.

Mayo, S. L., and R. L. Baldwin. 1993. Guanidinium chloride induction of partial unfolding in amide proton exchange in RNase A. *Science.* 262: 873–876.

Pershina, L., and A. Hvidt. 1974. A study by the hydrogen-exchange method of the complex formed between the basic pancreatic trypsin inhibitor and trypsin. *Eur. J. Biochem.* 48:339–344.

Privalov, P. L. 1979. Stability of proteins: small globular proteins. *Adv. Protein Chem.* 33:167–241.

Receveur, V., P. Calmettes, J. C. Smith, M. Desmadril, G. Coddens, and D. Durand. 1997. Picosecond dynamical changes on denaturation of yeast phosphoglycerate kinase revealed by quasielastic neutron scattering. *Proteins.* 28:380–387.

Roder, H. 1989. Structural characterization of protein folding intermediates by proton magnetic resonance and hydrogen exchange. *Methods Enzymol.* 176:446–473.

Susi, H. 1972. The strength of hydrogen bonding: infrared spectroscopy. *Methods Enzymol.* 26:381–391.

Tang, K. E., and K. A. Dill. 1998. Native protein fluctuations: the conformational-motion temperature and the inverse correlation of protein flexibility with protein stability. *J. Biomol. Struct. Dyn.* 16:397–411.

Vielle, C., and J. G. Zeikus. 1996. Thermoenzymes: identifying molecular determinants of protein structural and functional stability. *Trends Biotechnol.* 14:183–190.

Vihinen, M., and P. Mäntsälä. 1989. Microbial amylotytic enzymes. *Crit. Rev. Biochem. Mol. Biol.* 24:329–418.

Violet, M., and J.-C. Meunier. 1989. Kinetic study of irreversible thermal denaturation of *Bacillus licheniformis* alpha-amylase. *Biochem. J.* 263: 665–670.

Volino, F., and A. J. Dianoux. 1980. Neutron incoherent scattering law for diffusion in a potential of spherical symmetry: general formalism and application to diffusion inside a sphere. *Mol. Phys.* 41:271–279.

Wagner, G., and K. Wuthrich. 1979. Correlation between the amide proton exchange rates and the denaturation temperatures in globular proteins related to the basic pancreatic trypsin inhibitor. *J. Mol. Biol.* 130:31–37.

Wallon, G., G. Kryger, S. T. Lovett, T. Oshima, D. Ringe, and G. A. Petsko. 1997. Crystal structures of *Escherichia coli* and *Salmonella typhimurium* 3-isopropylmalate dehydrogenase and comparison with their thermophilic counterpart from *Thermus thermophilus*. *J. Mol. Biol.* 266:1016–1031.

Yamasaki, K., A. Akasako-Furukawa, and S. Kanaya. 1998. Structural stability and internal motions of *Escherichia coli* ribonuclease HI: ^{15}N relaxation and hydrogen-deuterium exchange analyses. *J. Mol. Biol.* 277:707–722.

Zavodszky, P., J. Kardos, Svingor, and G. A. Petsko. 1998. Adjustment of conformational flexibility is a key event in the thermal adaptation of proteins. *Proc. Natl. Acad. Sci. USA.* 95:7406–7411.